WEST-EAST HIGH SPEED FLOW FIELD CONFERENCE
19-22, November 2007
Moscow, Russia

SELF-OSCILLATORY REGIMES OF THE SONIC JET/FLAT PLATE INTERACTION: THEORETICAL PREDICTIONS VS. EXPERIMENTAL DATA

Michail G. Lebedev and Olga V. Bocharova

Moscow State University, Department of Computational Mathematics and Cybernetics
Leninskie Gory, 119992 Moscow, Russia
Email: somniac@rambler.ru, bocharova.olga@gmail.com

Key words: aeroacoustics, jet flows, choked jets, interaction with barriers, self-oscillations, Hartmann resonator, numerical simulation, Godunov method.

Abstract.
The Godunov method is applied to solve the time-dependent Euler equations for the case of the impingement of a round underexpanded sonic jet on a flat plate normal to the flow. Emphasis is placed on the self-oscillatory regimes of the interaction. The calculated flowfields and acoustic fields are compared with the experimental data of Powell, Henderson, Morch, Naberezhnova, and others. Both steady jet parameters, such as the geometrical structure of the jet and the flow parameter distributions, and acoustic parameters, such as the fundamental frequency of the self-oscillations obtained by the spectral analysis of the calculated time-dependent processes, are found to be in fairly good agreement with the measured data. Possible mechanisms of the generation of the self-oscillations and the production of sound are discussed.

One of the outstanding problems in aeroacoustics is the mechanism of the excitation and maintenance of self-oscillations occurring when an imperfectly expanded supersonic jet impinges on a barrier. J. Hartmann[1] was the first who observed, as long ago as in 1919, this phenomenon in his experiments in which a body with an upstream-facing cavity was embedded in an underexpanded, or "choked", sonic jet issuing from a convergent nozzle. The phenomenon received the name of the Hartmann resonator. Later, it was found that the self-oscillations can also be excited when the obstacle embedded in the jet flow represents not only a concave but also a convex body; the examples of such bodies are furnished by a sphere and a flat plate. Moreover, the self-oscillations were also observed in supersonic impinging jets, both underexpanded and overexpanded. However, in what follows all the flows of this type will be referred to as the Hartmann flows.

In succeeding years, many important features of the self-oscillatory impinging-jet flows were established and confirmed in numerous studies. Unfortunately, accumulation of the data did not result in a breakthrough in the understanding of the causes of the phenomenon. It can be said that this pedigreed puzzle has resisted about 90 years at experimental investigation, theoretical speculation, and numerical exploration. That it continues to draw the attention of many researchers is attributable to, at least, two

factors. Firstly, the fact itself that a physical problem is still incompletely understood arouses the excitement of scientists. Secondly, the phenomenon is widely used in engineering applications, in particular, for initiating and intensifying useful physical and chemical processes, for example, detonation in pulsed detonation engines (PDE)[2]. It should be noted that the occurrence of the self-oscillations accompanying the jet/barrier interaction can also be troublesome, as evidenced by a great number of publications in the United States in connection with the short takeoff and vertical landing (STOVL) problem.

When computer technologies and numerical methods had become the practice in the scientific, and, in particular, gasdynamic and acoustical research, the hopes of many researchers were pinned on the solution of the problem in numerical experiments. In fact, as early as at the end of the seventies of the last century the pioneering numerical study appeared. It was G. Naberezhnova who first succeeded in reproducing the self-oscillations accompanying the impingement of an underexpanded sonic jet on a flat plate[3]. Since then, many numerical studies were performed within the framework of the Euler, Navier-Stokes, and Reynolds equations. Here, we would like to mention only one study[4] remarkable for that it included numerical simulation performed using the first-, second-, and third-order difference schemes, the results obtained using these three approaches being about the same, both qualitatively and quantitatively. Thus, the plausibility of the numerical results concerning the Hartmann flow was confirmed. However, it could hardly be said that numerous numerical calculations carried out in the past brought us closer to the understanding of the mechanism of the Hartmann flow and similar phenomena. One of the reasons is restricted possibilities of computer technologies of even recent past.

At present, the computer capacities, that have considerably grown most recently, together with the parallel programming technologies and the modern techniques for processing the computer information, allow us to hope for the progress in the global solution of the problem.

In this study, we consider the interaction between a round sonic underexpanded ("choked") jet and a flat plate placed perpendicular to the jet axis.

The supersonic jet outflow into an ambient space is determined by the flow parameters at the nozzle exit and those in the surrounding. In the case of a uniform flow at the nozzle exit and the outflow into a medium at rest, within the framework of the inviscid gas model the problem is completely determined by the control parameters M_a, γ_a, γ_e, $N = p_a/p_e$, and $E = \rho_a/\rho_e$. Here, M_a, p_a, and ρ_a are the Mach number, the pressure, and the density at the nozzle exit, and γ_a and γ_e are the specific heat ratios of the gas issuing from the nozzle and that in the ambient space. The parameter N is the exit-to-ambient pressure ratio used usually in the Russian literature to characterize the gas expansion degree at the nozzle exit. At the same time, in the Western literature another parameter, namely, the nozzle pressure ratio (NPR) is usually used; NPR is the ratio of the stagnation pressure of the flow issuing from the nozzle to the surrounding pressure. For a sonic air jet N and NPR are related by a simple formula: $N = 0.528$ NPR.

Within the framework of the inviscid gas model the parameter E has no effect on the steady jet outflow, since the density (and temperature) difference across the jet boundary represented by a contact discontinuity may be arbitrary. Of course, when the viscous gas properties are taken into account, the flow is no longer independent of E, since this parameter influences the properties of the mixing layer which in this case takes the place of an infinitely thin jet boundary. We note that the parameter E can be

relevant even in the case of the inviscid model if time-dependent outflow is considered, in particular, the propagation of acoustic disturbances from an oscillating jet into the ambient space and the development of the feedback loop including the external acoustic field.

In this study, we consider the case of the sonic ($M_a = 1$) air jet outflow in the air ($\gamma_a = \gamma_e = 1.4$); the ratios N and E are the control parameters of the outflow. When a plane barrier, namely a flat plate of radius R', is placed in the jet, the resulting flow depends on two more dimensionless geometric parameters, namely, $R = R'/r_a$ and $L = l/r_a$, where l is the nozzle-to-plate spacing and r_a is the nozzle radius. We considered the cases of small-sized ($R = 1$) and large-sized ($R = \infty$) barriers, while the distance L was varied on a wide range.

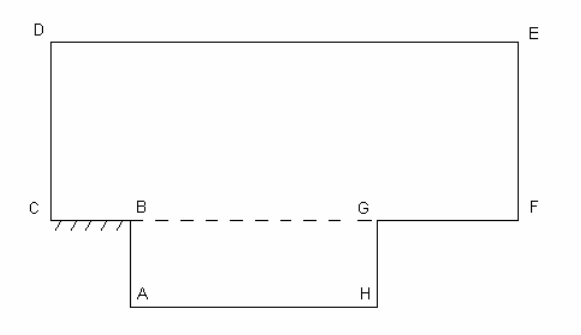

Figure 1. Computational domain

Figure 1 presents the computational domain. Points A and H lie on the x axis, while points C and D on the y axis; AB is the nozzle exit section, BC is the rigid side wall of the nozzle, HG is the flat endface of the cylindrical body, and GF is its lateral surface; when $R = \infty$, GH is absent. At the initial moment the flow parameters in the domain $ABCDEFGH$ are taken to be equal to those of the undisturbed ambient medium:

$$p_e = \frac{p_a}{N}, \rho_e = \frac{\rho_a}{E}, u_e = 0, v_e = 0, E = 1 \tag{1}$$

The boundary conditions imposed in the nozzle exit section are as follows:

$$p_a = \frac{u_a^2 \rho_a}{\gamma M_a^2}, \rho_a = 1, u_a = 1, v_a = 0 \tag{2}$$

The impermeability conditions are imposed on the side wall of the nozzle ($v = 0$), on the GF boundary ($v = 0$), and on the HG boundary ($u = 0$); at the axis of symmetry, the corresponding symmetry conditions are preassigned.

In accordance with the recommendations given in study[5], the boundary conditions with a bordering layer were imposed on the outer, artificial boundaries CD, DE, and EF of the computational domain. In opinion of the authors of study[5], precisely these conditions make it possible adequately to describe the solution with outgoing waves at the boundaries of the computational domain.

The problem thus formulated was solved numerically by the well-known Godunov method[6]. The calculations were carried out using the 16-processor SMP system Regatta – IBM eServer p690. In the case of large grids the parallelization of the algorithm made

it possible to reduce the required computation time by an order as compared with the single-processor realization.

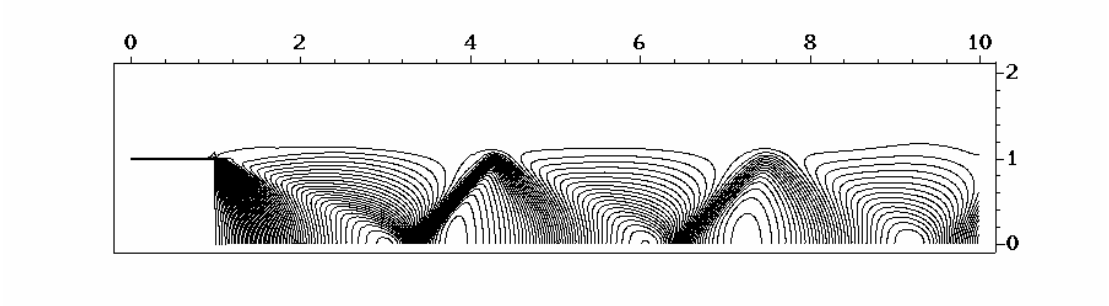

Figure 2. Flow pattern in the free jet (N=**2**)

The calculated flow pattern for a free (no barrier) jet is presented in Fig. 2 (the pressure contours are plotted). Here, the periodic, or cellular, jet structure, that consists of incident and reflected shock waves, is clearly visible. We note that in the outflow regime under consideration the lip shock reflection from the axis of symmetry is quasi-regular (or pseudoregular): the Mach disk radius is vanishingly small. The reflection point coordinate is $x \approx 3.4$. The calculated results are in good agreement with the experimental data[7] on the positions of the points of intersection of the internal shock waves with the axis of symmetry. In Fig. 3 the calculated and measured[8] Mach number profiles along the jet axis are compared. These also agree well, though the measured profile is somewhat smoother than the calculated one, owing apparently to the effect of dissipation processes.

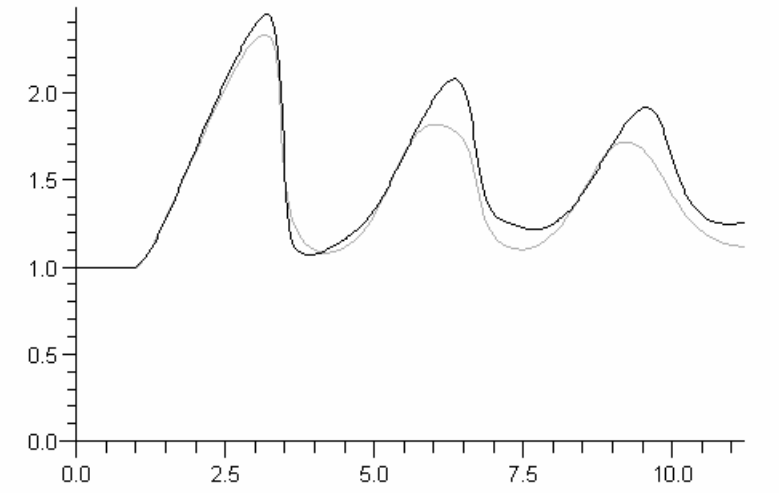

Figure 3. Mach number profile along the free jet axis (N = **2**). Calculated (dark) and measured (gray) results.

We are now coming to the case of the jet flow around a small-sized barrier, namely, a flat-ended circular cylinder of radius $R = r_a$. The calculations showed that on a fairly narrow nozzle-to-plate spacing range $2.7 < l/r_a < 3.7$ the flow is characterized by undamped fluctuations. An example of these fluctuations is shown in Fig. 4 which presents the time dependence of the pressure at the stagnation point on the disk. The most intense fluctuations were observed for $l/r_a = 3.2$. This barrier position corresponds

to the end of the first cell ("barrel") of the undisturbed jet. Spectral analysis of the time dependence of the flow parameters made it possible to separate out the fundamental tone of the fluctuations.

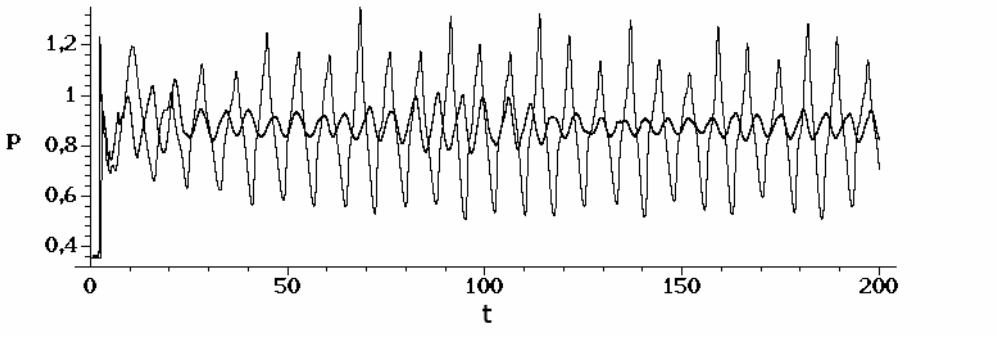

Figure 4. Time dependence of the pressure at the centre of the plate for N = **2,** L = **2.7** and L = **3.2**

Figure 5 presents, along with the time dependences of the stagnation-point pressure for $l = 3.2r_a$ and $l = 3.5r_a$, the self-correlation functions associated with the time-dependent processes $p(t)$ and the frequency distributions of the spectral density.

$$k(\tau) = \lim_{T\to\infty} \int_0^T p(t)\,p(t+\tau)dt,$$
$$S(\omega) = 2\int_0^\infty k(\tau)\cos(\omega\tau)d\tau. \qquad (3)$$

Obviously, the most intense fluctuations observed for l/r_a = 3.2 are rather regular, so that the self-correlation function is near-sinusoidal and the fluctuation spectrum is characterized by a single peak with a fairly large amplitude (its value measured in conditional units is about 40). Contrariwise, the fluctuations corresponding to the boundary region of the undamped oscillation range (l/r_a = 3.5) become less intense and rather chaotic; in this case, the frequency spectrum includes several closely-spaced peaks, the amplitude of the largest peak being equal to about 13.

The calculated frequencies (wavelengths) of the self-oscillations occurring, when a sonic underexpanded jet impinges on plates of different dimensions, are compared with the experimental data in Fig. 6; in all the cases considered the barrier diameter is less than, equal to, or of the same order as the nozzle exit diameter. The self-oscillations wavelengths measured in the experiments [7, 9, 10] for different but similar in value plate dimensions lie practically on the same line (in the log coordinates). The calculated dependence of the self-oscillation wavelength on the nozzle-to-barrier spacing is also presented by a straight line with the same slope as the experimental one, though lying somewhat higher (by about 10%; it should be borne in mind that this figure is, as it were, upturned, since the λ axis is downward directed). The systematic deviation of these two lines can be attributed to the fact that the calculations were performed for a slightly heated jet with the exit-to-ambient temperature ratio T_a/T_e = 1, while the experiments had been, apparently, carried out on cold air jets ($T_a/T_e \approx 0.8$).

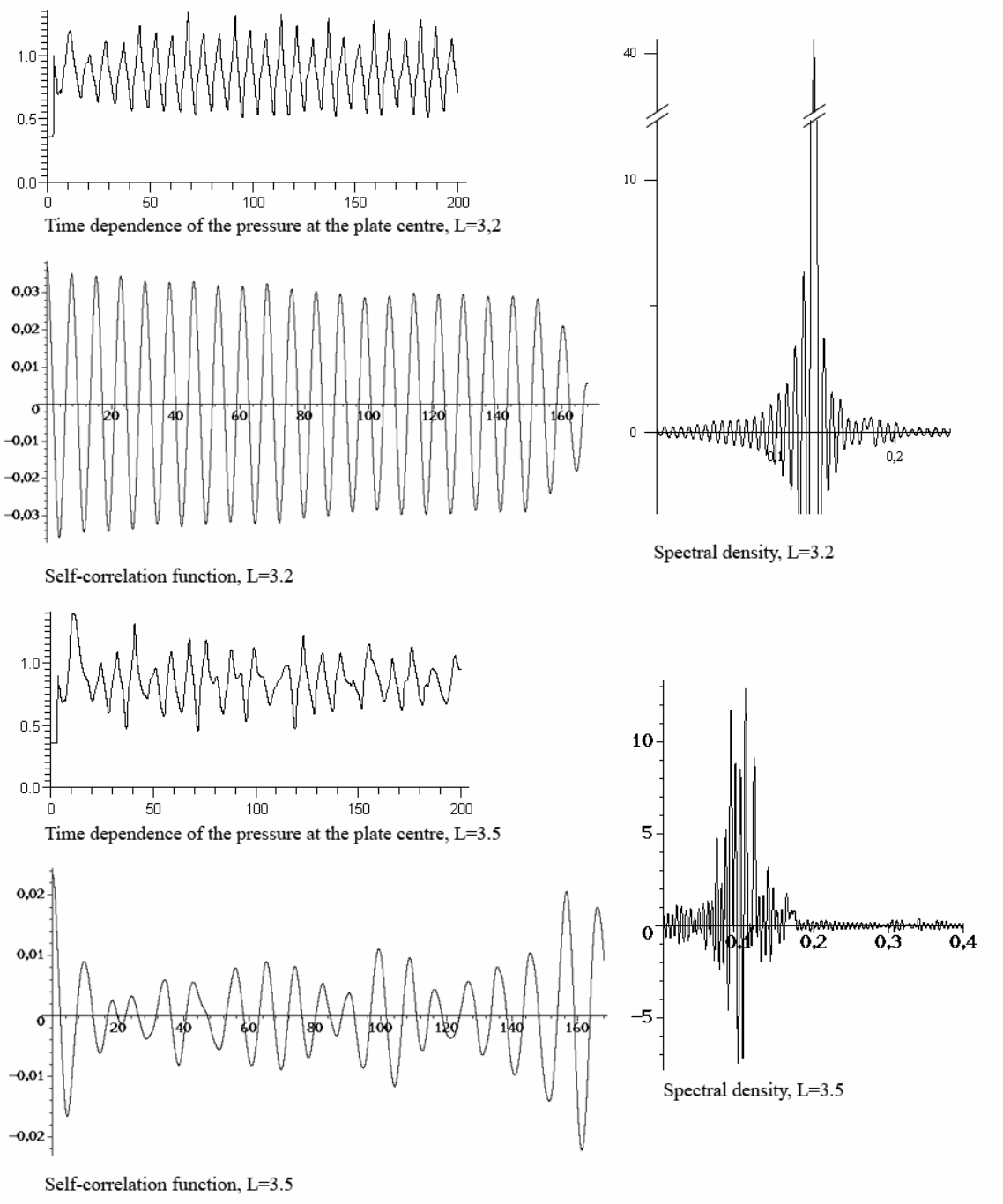

Figure 5. Spectral characteristics of self-oscillation process for N = **2,** L = **3.2** and L = **3.5**

The vertical dashed lines on the plot indicate the approximate boundaries of the nozzle-to-plate spacing range on which the self-oscillations occur; these ranges coincide in the calculations and the experiment[7].

Figures 7 to 10 present separate snapshots of the animated movies created by processing the calculated results. They make it possible to trace the evolution of the flow pattern during one period of the oscillatory motion in the case in which $N = 2$, $R/r_a = 1$, and $L/r_a = 3.2$. In the figures, the pressure and Mach number contours and the velocity fields are plotted, together with the profiles of the longitudinal velocity along the axis of symmetry and the pressure along the spreading line of the flow. Clearly visible in the

figures are time-dependent rarefaction and compression waves that arise upon the interaction between the bow shock ahead of the barrier and the jet boundary.

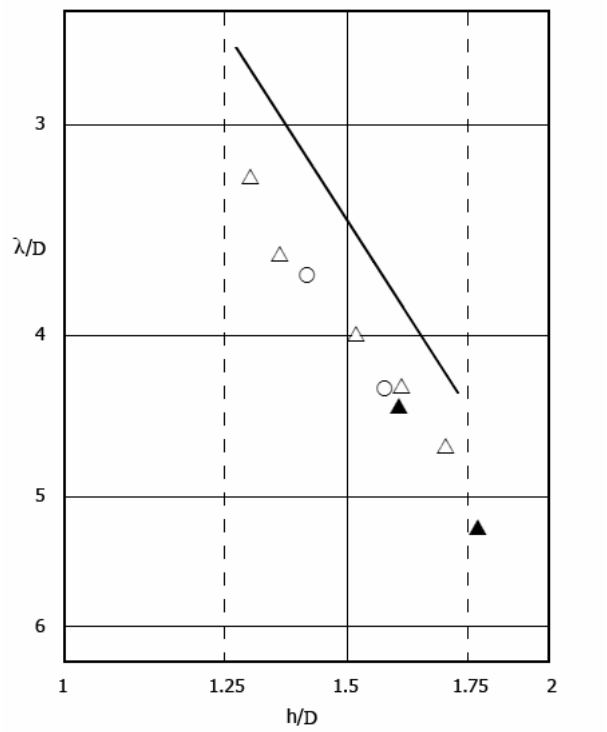

Figure 6. Comparison of the calculated and measured data on the frequency (wavelength) of the sonic underexpanded impinging jet fluctuations (N = **2**). ─ Calculation, $d = D/D_a$ = **1**; △ [7], d = **1**; ▲ [9], d = **0.58**; ○ [10], d = **1.1**

At the rightmost position of the bow shock, which corresponds to the closest approach to the plate (Fig. 7), the shock vertex is located approximately at the point of intersection of the lip shock in the undisturbed jet with the axis of symmetry (cf. Figs. 2 and 7). At this moment, the pressure at the plate center reaches its maximum (over the period) value. The pressure distribution over the surface is near-uniform. Then (Fig. 8) the pressure at the barrier starts to decrease, with the formation of a slight pressure peak near the barrier edge. The velocity at the axis of symmetry becomes negative in the vicinity of the barrier. The bow shock moves toward the nozzle. A recirculation (return flow) zone is formed in the shock layer ahead of the barrier. In the process of this motion, when the bow shock has not yet reached its leftmost position, a new, annular, shock starts to form in the jet, near the corner point of the plate (it looks like a small dash perpendicular to the axis of symmetry). Apparently, its formation is due to the reflection of the rarefaction fan proceeding of the point of intersection of the bow shock with the jet boundary from the discontinuity line within the shock layer proceeding of the point of intersection of the bow shock with the lip shock in the jet. As it grows in size extending along the y axis, the return flow zone shrinks.

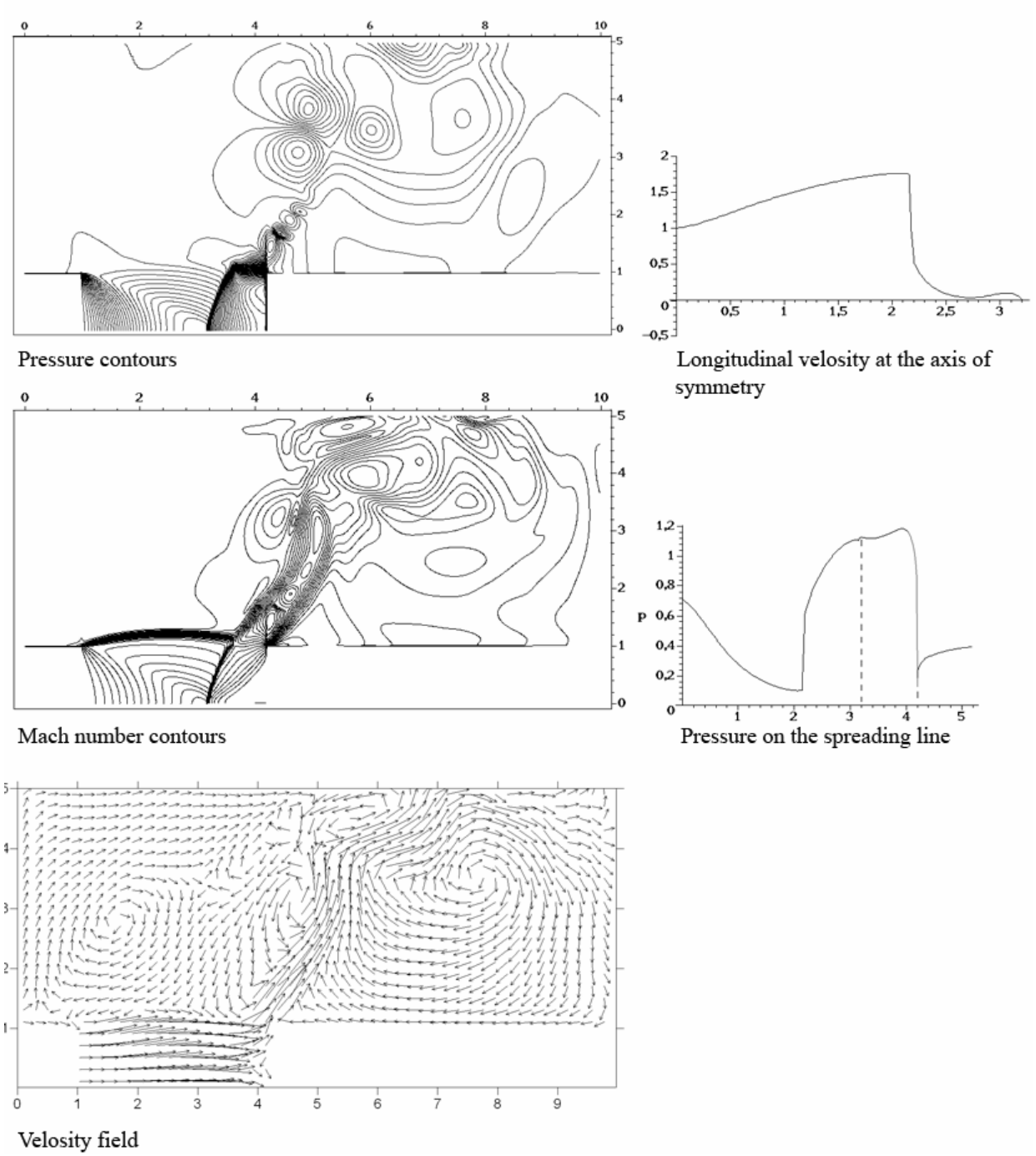

Figure 7. Snapshot of the jet/barrier interaction at t = **120.94**

In Fig. 9 the bow shock is at the leftmost position. In this case, the pressure behind the bow shock is greater than that at the nozzle exit which, in turn, is greater than that at the barrier. In this snapshot the flow pattern is especially well-defined. Ahead of the barrier there is a near-conical dead-air zone with a low-velocity recirculation flow. The lateral surface of the zone and the jet boundary after the point of its intersection with the bow shock form the boundaries of an annular stream that starts within the shock layer ahead of the plate. On leaving the shock layer, this stream continues to flow in the form of a narrow annular jet inclined at a certain angle to the axis of symmetry. The jet possesses a clearly-cut cellular structure formed by internal shock waves of which the above-mentioned annular shock is the first. The angles of inclination of different cells to the axis of symmetry are different and time-dependent, so that the jet looks like a polygonal

line whose links oscillate one about another; it is interesting to note that the fifth cell of the jet is near-perpendicular to the axis of symmetry.

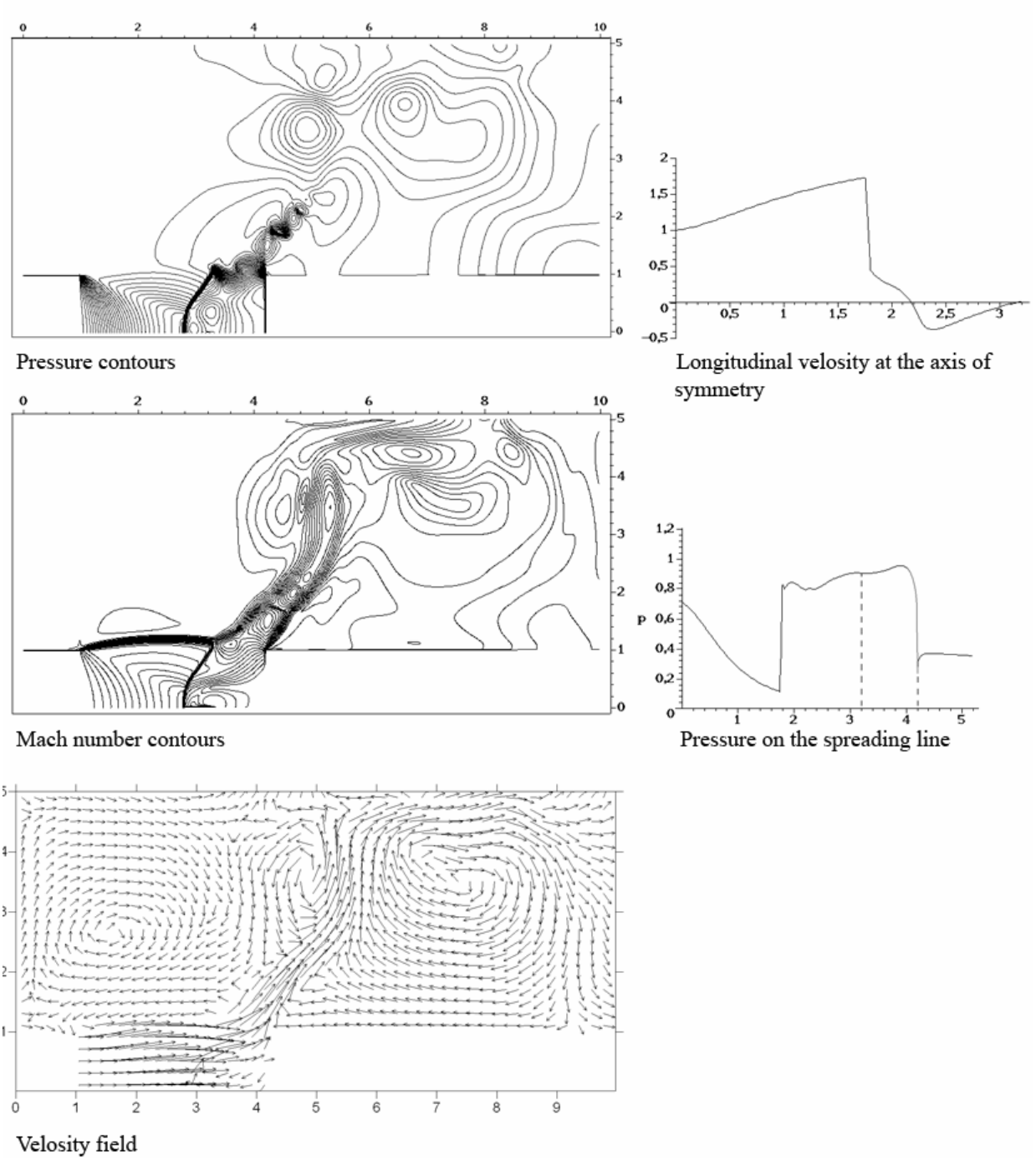

Figure 8. Snapshot of the jet/barrier interaction at t = **122.84**

The jet divides the flowfield into two parts, upstream and downstream; in both parts low-velocity vortex flows are formed. The positions of the centers of the vortices vary with time; along with these main, large-scale vortices, on the upstream side there also exist several small-scale vortices adjoining the annular jet boundary. The vortices are so oriented that near the main jet boundary the flow in the ambient space is downward directed. We note that this downward-directed flow can have an effect on the maintenance of the self-oscillations.

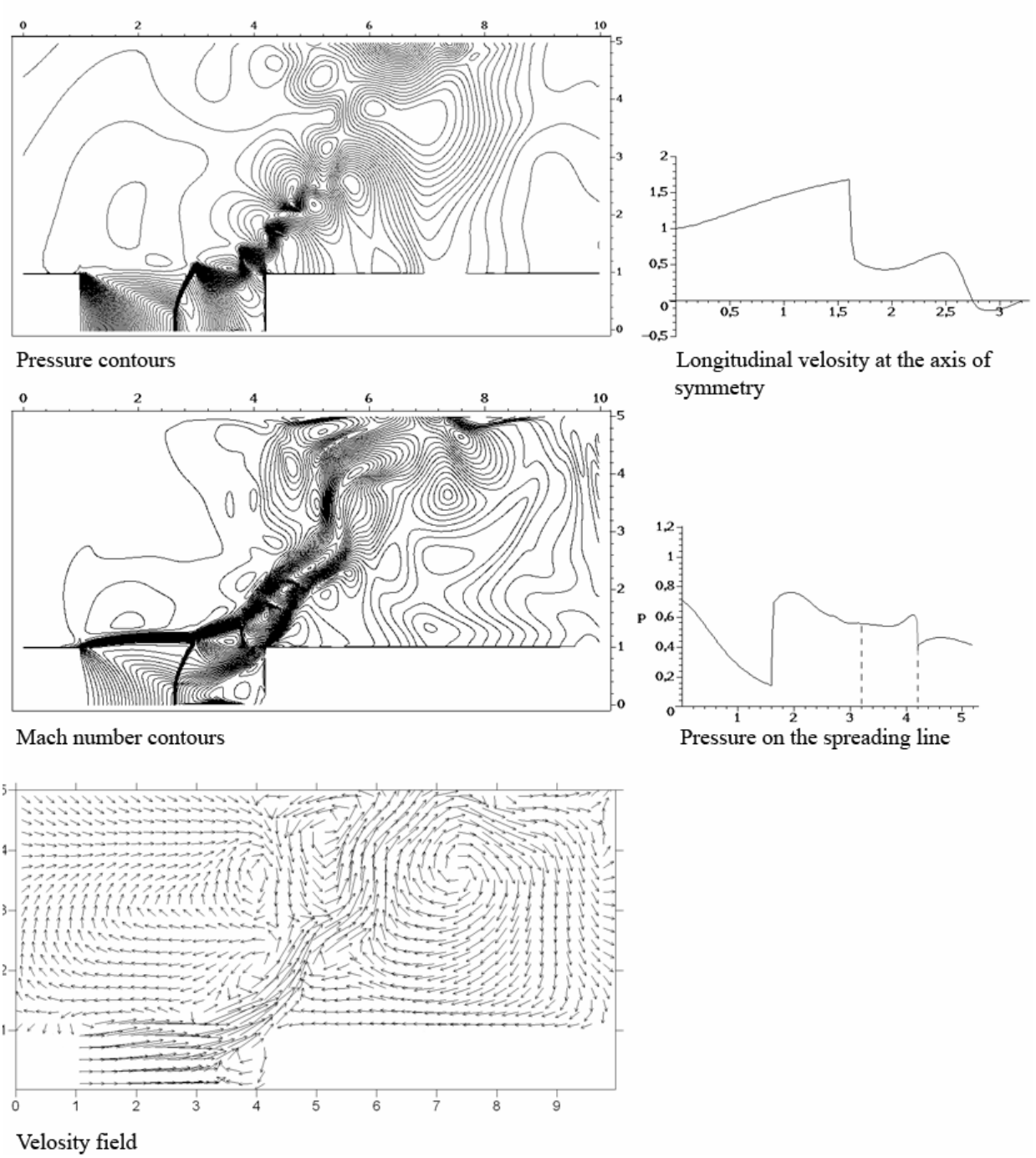

Figure 9. Snapshot of the jet/barrier interaction at t = **124.76**

When the bow shock is at the leftmost position, ahead of it there is an accelerated flow of the jet core which prompts the shock to regain its original position (Fig. 10). On its return trip the bow shock coalesces with the above-mentioned annular shock; the moment of the coalescence corresponds to the rightmost position of the bow shock. Then the process is repeated: the motion to the left, that is, toward the nozzle, starts again. The bow shock is always dome-shaped; it is more convex when it is displaced from the rightmost to the leftmost position than during the return travel.

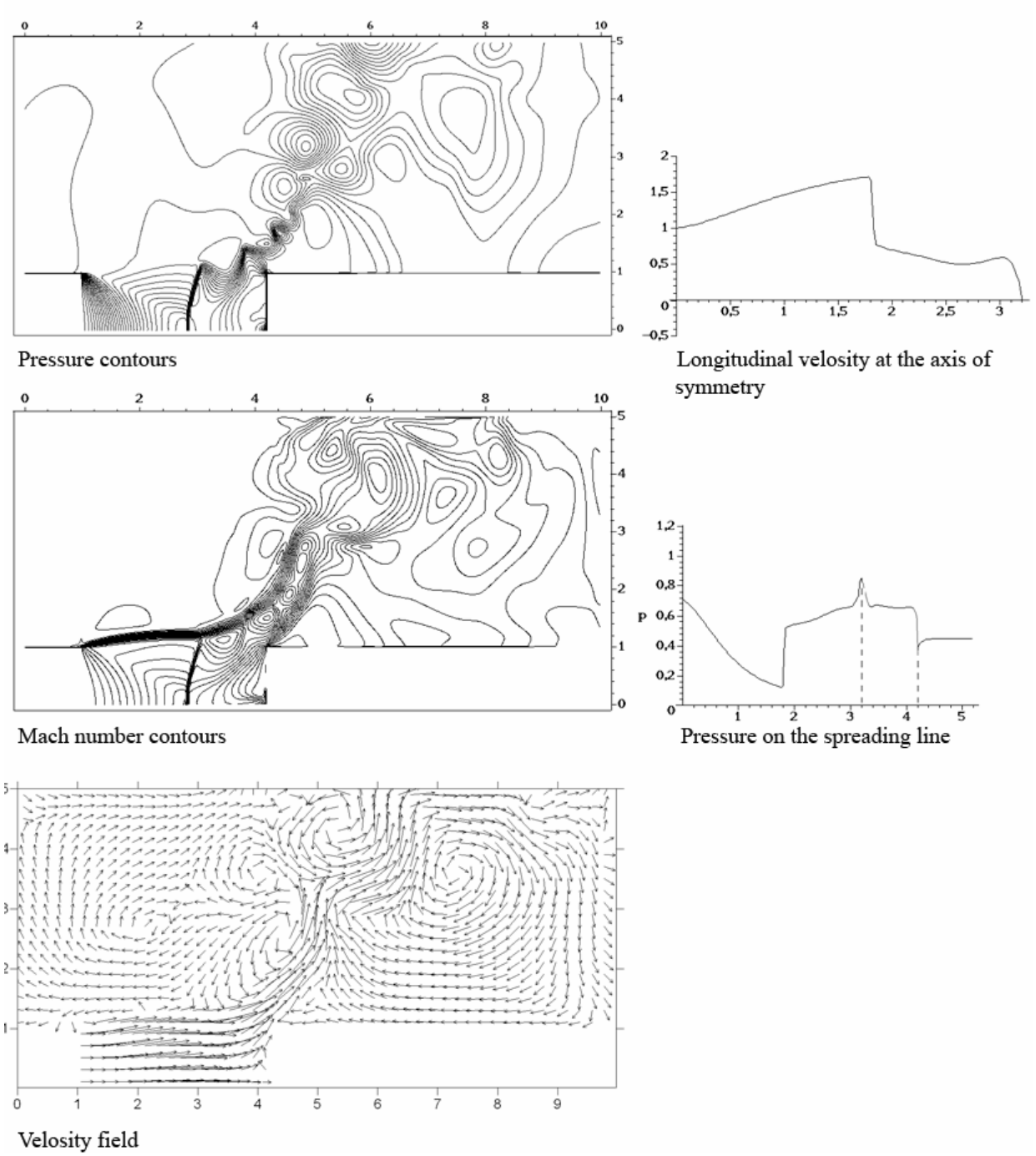

Figure 10. Snapshot of the jet/barrier interaction at t = **126.65**

The main stages of the oscillatory process, as described above, are in qualitative agreement with the flow visualization data obtained in study[8], in which, in particular, the formation of the annular shock, its travel along the shock layer, and the disappearance (coalescence with the bow shock) were observed. As for the return flow zones in the vicinity of the axis of symmetry, these were observable in many experimental studies. The presence of these zones and the nonmonotonic nature of the pressure distribution over the barrier characterized by a peripheral peak was proposed by many authors as the main factor responsible for the occurrence of the self-oscillations. However, it can hardly play the key role in the process, since the dimensions of the recirculation zone in the vicinity of the stagnation point are not large and the excess of the pressure at the plate periphery over that at the stagnation point is

not high. We note that study[8] presents a detailed overview of the experimental data concerning the occurrence of the recirculation zones and self-oscillations in impinging jets. It turned out that there is no clear-cut relation between the two phenomena. This means that self-oscillations can occur in the absence of the recirculation zones and, on the contrary, steady circulatory flow patterns are also possible.

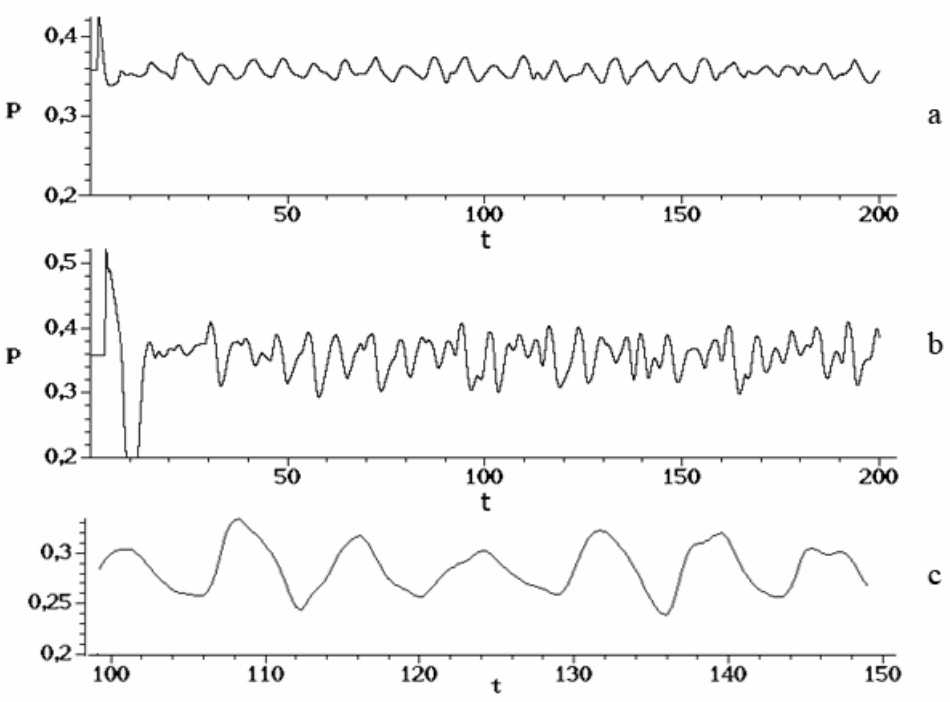

Figure 11. Acoustic disturbances in the external field [x = **1**, y = **2.5** (a) and x = **4.2**, y = **2.5** (b)] and inside the jet [x = **2.4**, y = **0.8** (c)] N = 1, L = **3.2**

The jet oscillations lead to the radiation of acoustic disturbances in the ambient space. In Fig. 11 we have plotted the time dependence of the pressure at two points of the external acoustic field; both points are located at a distance $y = 2.5r_a$ above the axis of symmetry, in the exit section plane ($x = 1r_a$) and in the plane of the barrier ($x = 4.2r_a$). The periodic nature of the time dependence of the pressure is obvious; the frequency of the oscillations is the same as that of the pressure at the stagnation point on the barrier. In the former case, the amplitude of the fluctuations amounts to 10-15% of the undisturbed (atmospheric) pressure and is even higher in the latter case.

The acoustic disturbances in the external space affect, in turn, the jet flow. The pressure fluctuations are observable, for example, at point $x = 2.4r_a$, y = $0.8r_a$, that is, within the jet and ahead of the oscillating bow shock. However, whether these fluctuations represent a part of the feedback loop responsible for the occurrence of the self-oscillations, remains unclear. We performed a numerical experiment with a rigid screen placed in the external acoustic field. The annular screen with an only narrow gap between the jet boundary and the screen edge was introduced at a distance x = 3 (Fig. 12) for the purpose of interrupting the loop. However, as can be seen form Fig. 12, introducing the screen has almost no effect on the fluctuations of both the pressure at the plate and the jet shape.

Thus, the analysis of the calculated results for the self-oscillations in the impinging jets (at least, in the particular case of a small-sized barrier embedded in the sonic choked jet) favors neither the hypothesis that the self-oscillations are maintained by the feedback loop in the external acoustic field nor that they are caused by recirculation flows within

the shock layer. A possible explanation of the phenomenon can be provided by flow-rate fluctuations that arise when the bow shock ahead of the barrier turns out to be located at the seat of a drastic change in the jet flow structure. In fact, when the bow shock is in the rightmost position (Fig. 7) the oncoming flow is decelerated across the lip shock in the jet and a small shock-layer thickness can turn out to be insufficient to permit the passage of the corresponding gas flow rate. The bow shock moves from the barrier toward the nozzle (Figs. 8 and 9) but now the oncoming flow is the accelerated jet core flow which brings the bow shock back to its original position (Fig. 10). It can turn out that an equilibrium position is not attained and the process is repeated. However, the elucidation of the self-oscillation mechanism calls for further detailed investigation.

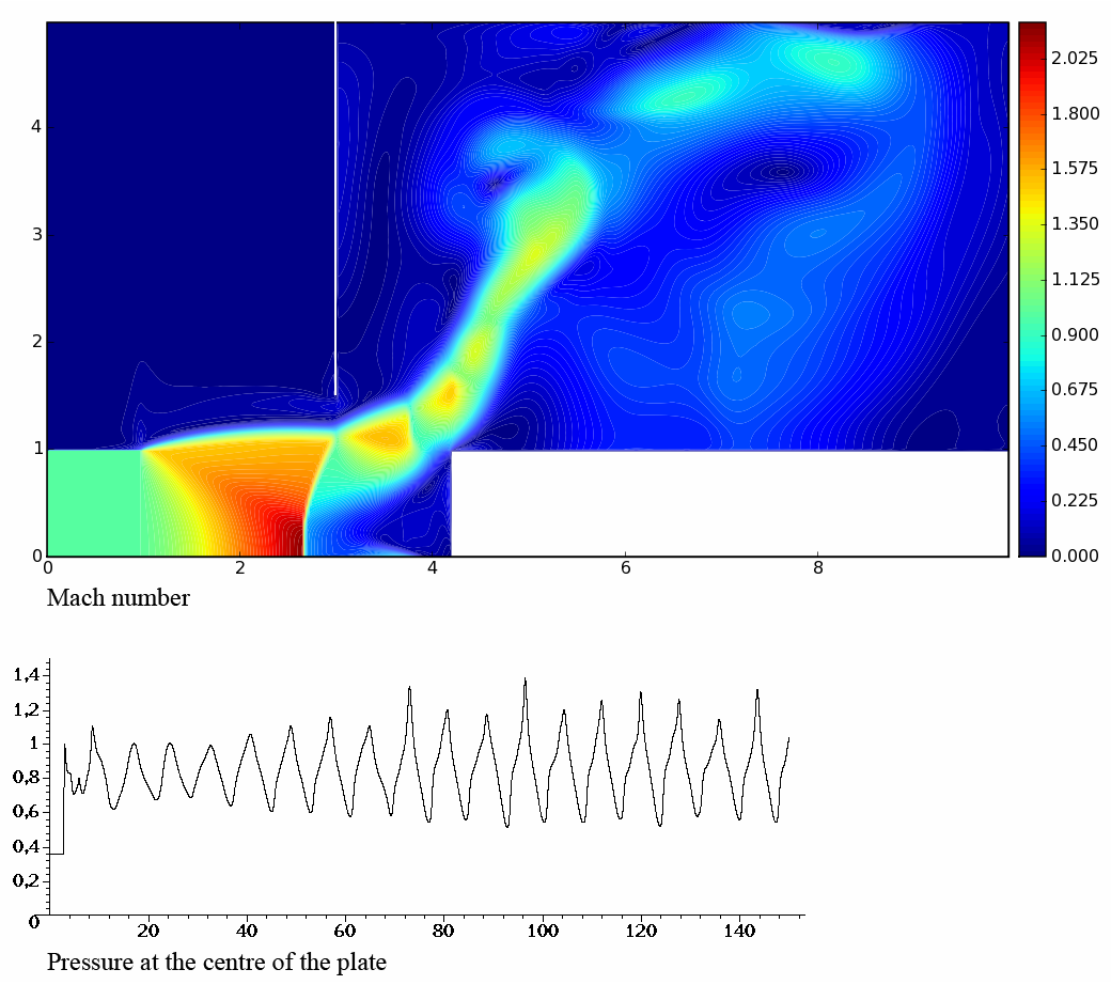

Figure 12. Self-oscillations in the presence of an annular screen in the external acoustic field (N=**2**, L=**3.2**)

An example of the calculation of the impingement of the sonic jet on an infinite plate is presented in Fig. 13. Clearly, the pressure at the plate center executes fairly regular oscillations. In the same figure, two snapshots of the flowfield are given; they correspond to the leftmost and rightmost positions of the oscillating bow shock.

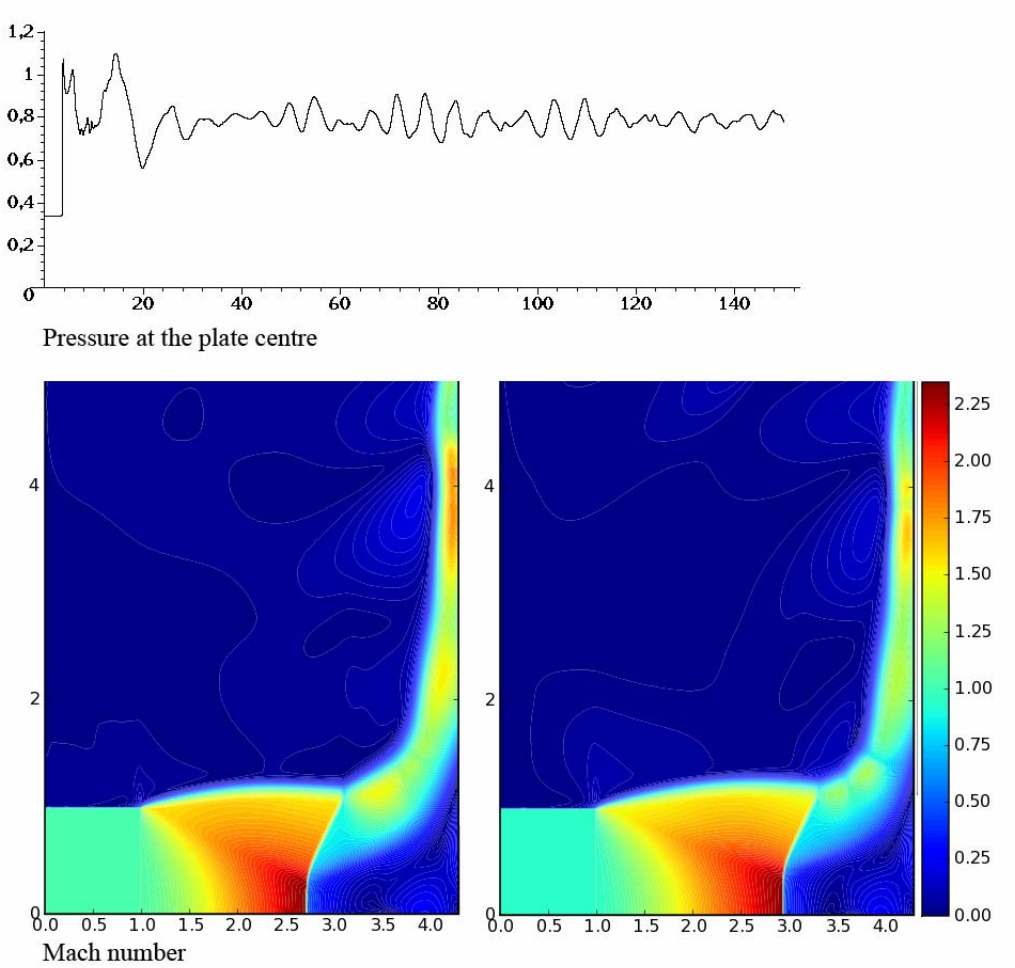

Figure 13. Impingement of the sonic jet on an infinite plate (N = **2**, L = **3.3**)

REFERENCES

[1] J. Hartmann, "On a new method for the generation of sound waves", *Phys. Rev*, 20, 719-727 (1922).

[2] V.A. Levin, Yu.N. Nechaev, and A.I. Tarasov, "A new approach to organizing operation cycles in pulsed detonation engines", *Int. Colloq. on Control of Detonation Processes, 4-7 July, 2000, Moscow, Russia* (2000).

[3] G.V. Naberezhnova, "Calculation of the unsteady interaction of a supersonic jet with a plane barrier by the large particle method", *Tr. TsAGI*, No. 1899, 31-42 (1978).

[4] V.B. Bazarov, G.S. Roslyakov, Yu.N. Sadkov, and M.V. Shustova, "Supersonic imperfectly expanded jets and their interaction with barriers," *Mat. Model.*, 8, No. 6, 19-32 (1996).

[5] A.N. Kraiko and K.S. Pyankov, "Ideal gas flows with separation zones and unsteady contact discontinuities of complicated shapes", *Izv. Ross. Akad. Nauk. Mekh. Zhidk. Gaza*, No. 5, 39-54 (2006).

[6] S.K. Godunov, A.V. Zabrodin, M.Ya. Ivanov, A.N. Kraiko, and G.P. Prokopov, *Numerical Solution of Multi-Dimensional Problems of Gas Dynamics* [in Russian], Nauka, Moscow (1976).

[7] A. Powell, "The sound-producing oscillations of round underexpanded jets impinging on normal plates", *J. Acoust. Soc. Am.*., 83, 515-533 (1988).

[8] B. Henderson, J. Bridges, and M. Wernet, "An experimental study of the oscillatory flow structure of tone-producing supersonic impinging jets", *J. Fluid Mech.*, 542, 15-137 (2005).

[9] K.A. Morch, "A theory of the mode of operation of the Hartmann air jet generation", *J. Fluid Mech*., 20, 141-159 (1964).

[10] G.V. Naberezhnova and Yu.N. Netsterov, "Investigation of the pressure fluctuations on a plane barrier placed in an underexpanded jet perpendicular to its axis",*Tr. TsAGI*, No. 1589, 3-17 (1974).